

A Natural Inactivating Mutation in the CovS Component of the CovRS Regulatory Operon in a Pattern D *Streptococcus pyogenes* Strain Influences Virulence-associated Genes^{*[5]}

Received for publication, December 5, 2012, and in revised form, December 28, 2012. Published, JBC Papers in Press, January 13, 2013, DOI 10.1074/jbc.M112.442657

Zhong Liang¹, Yueling Zhang¹, Garima Agrahari, Vishwanatha Chandрахas, Kristofor Ginton, Deborah L. Donahue, Rashna D. Balsara, Victoria A. Ploplis, and Francis J. Castellino²

From the W. M. Keck Center for Transgene Research and Department of Chemistry and Biochemistry, University of Notre Dame, Notre Dame, Indiana 46556

Background: The two-component CovRS system is a GAS virulence gene regulator.

Results: A natural inactivating mutation has been found in CovS in a skin-invasive GAS strain, potentially affecting expression of key virulence genes.

Conclusion: The mutation in CovS showed substantial effects on regulation of virulence genes.

Significance: Expression of genes critical to GAS virulence can reveal reasons why specific strains of GAS are effective tissue specialists.

A skin-tropic invasive group A *Streptococcus pyogenes* (GAS) strain, AP53, contains a natural inactivating mutation in the *covS* gene (*covS^M*) of the two-component responder (CovR)/sensor (CovS) gene regulatory system. The effects of this mutation on specific GAS virulence determinants have been assessed, with emphasis on expression of the extracellular protease, streptococcal pyrogenic exotoxin B (SpeB), capsular hyaluronic acid, and proteins that allow host plasmin assembly on the bacterial surface, *viz.* a high affinity plasminogen (Pg)/plasmin receptor, Pg-binding group A streptococcal M protein (PAM), and the human Pg activator streptokinase. To further illuminate mechanisms of the functioning of CovRS in the virulence of AP53, two AP53 isogenic strains were generated, one in which the natural *covS^M* gene was mutated to WT-*covS* (AP53/*covS^{WT}*) and a strain that contained an inactivated *covR* gene (AP53/ Δ *covR*). Two additional strains that do not contain PAM, *viz.* WT-NS931 and NS931/*covS^M*, were also employed. SpeB was not measurably expressed in strains containing *covR^{WT}/covS^M*, whereas in strains with natural or engineered *covR^{WT}/covS^{WT}*, SpeB expression was highly up-regulated. Alternatively, capsule synthesis via the *hasABC* operon was enhanced in strain AP53/*covS^M*, whereas streptokinase expression was only slightly affected by the *covS* inactivation. PAM expression was not substantially influenced by the *covS* mutation, suggesting that *covRS* had minimal effects on the *mga* regulon that controls PAM expression. These results demonstrate that a *covS* inactivation results in virulence gene alterations and also suggest that the CovR phosphorylation needed for gene up- or down-regulation can occur by alternative pathways to CovS kinase.

The Gram-positive bacterium, *Streptococcus pyogenes* (or GAS),³ is the causative agent for a number of human infections. These common human pathogens colonize epithelial cells of the throat and the epidermal layer of skin, causing an array of mild to very severe diseases, ranging from simple pharyngitis to life-threatening necrotizing fasciitis and toxic shock syndrome. Serious sequela of GAS infections include post-streptococcal glomerulonephritis and rheumatic fever. More than 250 types of GAS have been identified based on serotyping of ubiquitously expressed cell wall-anchored M-proteins (1), which are major GAS virulence protein products of *emm*-type genes. The *emm* and *emm*-like genes are present in a major core virulence region under transcriptional control of a single-component upstream transcriptional regulator (2) encoded by the *mga* gene (3). The protein expression product of *mga* coordinately activates a number of core cell surface primary virulence genes. Included in this group are genes encoding M-protein and other homologous genes, *e.g.* *fcR* and *enn*, the products of which bind to the Fc regions of IgG and IgA (4), respectively, along with complement-inactivating C5a peptidase, encoded by the gene *scpA* (5) and the product of the *fbp* gene that allows adhesion of the bacteria to host fibronectin (6). The proteins produced by these genes assist the GAS in overcoming innate immune-based opsonization of the bacteria by macrophages and polymorphonuclear cells and/or anchor the bacteria to host cellular components (7), thus promoting their invasive properties.

³ The abbreviations used are: GAS, group A streptococcus; SOF, serum opacity factor; *cat*, chloramphenicol acetyltransferase; h, human; Pg, plasminogen; Pm, plasmin; *covRS*, two-component cluster of virulence (Cov) sensor (S) and gene regulator (R); *emm*, a gene family encoding M-proteins; *sen*, streptococcal enolase gene; *gapdh*, glyceraldehyde-3-phosphate dehydrogenase gene; *plr*, gene encoding plasmin(ogen) receptor; *mga*, multiple gene regulator; *fcR*, gene coding IgG Fc receptor; *pam*, hPg-binding M-like protein gene; *enn*, gene encoding IgA Fc receptor; *scpA*, C5a peptidase gene; *fbp*, fibronectin-binding protein gene; *lbp*, laminin-binding protein gene; *mutS*, *dam*-directed mutator S gene; *hasABC*, hyaluronic acid synthetase operator; *speB*, streptococcal erythrogenic toxin B gene; SK, streptokinase; TMB, tetramethylbenzidine; *em^r*, erythromycin resistance gene; SCO, single crossover; DCO, double crossover; Q-RT, quantitative RT; FCA, flow cytometric analysis; r, recombinant.

* This work was supported, in whole or in part, by National Institutes of Health Grant HL013423 (to F. J. C.).

[5] This article contains supplemental Tables 1 and 2.

¹ Z. L. and Y. Z. contributed equally to this work.

² To whom correspondence should be addressed. Tel.: 574-631-8996; Tel./Fax: 574-631-8017; E-mail: fcastell@nd.edu.

Inactivating Mutation in *CovS* Component of *CovRS* Operon

In addition to these cell surface-associated virulence factors, a variety of GAS exoproducts are employed to promote virulence of the bacteria (8). One such example is streptokinase (SK), encoded by the bacterial *sk* gene. SK activates the critical host virulence factor human (h) plasma plasminogen (hPg), thus generating the fibrinolytic protease plasmin (hPm). This step assists in dissemination of the bacteria from local sterile fibrin-encased sites to deep tissue loci, the bloodstream, and the lymphatic system (9), and the invasiveness of GAS isolates has been correlated with direct binding of hPg/hPm to GAS (10). Subclasses of M-proteins have been shown to bind Pg/Pm directly (e.g. Pg-binding group A streptococcal M (PAM)-like protein-containing strains) (11) or indirectly via fibrinogen/fibrin-binding proteins, in each case allowing the bacteria to assemble a proteolytic surface (10). Although other streptococcal hPg/hPm receptors, e.g. the products of the *sen* and *plr* genes (12, 13), have been identified, their pathophysiological importance is unclear, especially in strains that produce functional PAM.

Two-component gene regulatory systems also exist in bacteria. In GAS, ~13 such regulators are known (14), the most studied of which is the intracellular cluster of virulence (*Cov*) OmpR-like responder (*covR*) (15), together with the cell surface-bound EnvZ-type *Cov* sensor (*covS*) (16) system, two genes that are adjacent to each other on the GAS genome and are cotranscribed from a single promoter upstream of *covR* (17). Available evidence suggests that membrane-bound *CovS* functions as an autophosphorylase, kinase, and/or phosphatase (18), phosphorylating or dephosphorylating the cognate responder, *CovR*, to modulate the *CovR*-based repression of genes that are needed for GAS survival in response to host pressure, e.g. host temperature elevation (16). It has been reported that a relationship exists between *CovRS* and *mga* gene regulation (6), in this way greatly expanding the number of genes regulated by *CovRS*.

We find herein that skin-invasive AP53 and NS931 strains of GAS possess a similar arrangement of genes in the *mga* core regulon. However, the *emm* genes producing M-protein in these strains contain important differences. AP53 expresses the *emm*-like gene encoding PAM that specifically interacts with a binding locus within hPg/hPm (19), in this manner capturing host proteins to promote focal activation of hPg by bacterially secreted SK (20) to generate a cell-bound extracellular protease, hPm. We show that WT-NS931 contains a form of M-protein that does not specifically interact with hPg/hPm. During the course of our work, we discovered a natural inactivating gene mutation in the sensor component, *covS*, of *covRS* in WT-AP53 cells that was not present in NS931 cells, and we undertook an investigation of the relationship between this mutation and the nature of the virulence genes that are expressed by these GAS strains, especially those that assist in assembling hPm on the bacterial cell surface. The results of these studies are the subject of this report.

EXPERIMENTAL PROCEDURES

Bacterial Strains—All *S. pyogenes* strains were originally collected as primary isolates. The parental PAM⁺ isolate, AP53 (21), and the PAM⁻ isolate, NS931 (10), have been described in

previous studies. These strains were provided by Dr. M. J. Walker (Queensland, Australia) and Dr. M. Sanderson-Smith (Wollongong, Australia).

Isolation of Genomic DNA (gDNA)—Single colonies of the *S. pyogenes* strains were picked from streaks on horse blood agar and grown in THY (Todd-Hewitt broth supplemented with 1% (w/v) yeast extract) overnight at 37 °C. gDNA was isolated after treatment of the cells with lysozyme/proteinase K and cell lysis buffer (100 mM Tris, 5 mM EDTA, 0.2% SDS, 200 mM NaCl, pH 8.5) and extracted with phenol/chloroform/isoamyl alcohol (25:24:1, v/v/v). The gDNA was precipitated with isopropyl alcohol and washed with 70% ethanol.

Gene Sequencing and Identification—Traditional Sanger sequencing was accomplished on an ABI 3730xl 96-capillary sequencer using custom-designed primers. Genes were identified and assigned by BLAST searches.

Construction of Isogenic GAS Strains Containing Targeted Mutations of GAS Genes—To construct gene-deleted (Δ) mutants, targeting vectors for genes of AP53 and NS931 cells were constructed with the chloramphenicol acetyltransferase (*cat*) gene 5'-flanked by 300–400 bp of DNA upstream of the ATG for the gene of interest and 3'-flanked by 300–400 bp downstream of the TAA/TAG stop codon for the same gene. Restriction sites (typically 5'-NotI and a 3'-Sall) were cloned into the two ends of the entire DNA segment and were used for insertion into the same sites of the temperature-sensitive plasmid, pHY304 (from M. J. Walker), which also contained the erythromycin resistance (*emr*) gene. The resulting plasmid was then transformed into cells of interest by electroporation. Chromosomal integration via allelic replacement (22) was achieved by single crossover (SCO) at 30 °C for plasmid replication and then switched to 37 °C overnight for screening for Em^r. For confirmation, SCO⁺ mutants were further screened by PCR with primers internal to the *emr* gene. The confirmed SCO⁺ cells were replicated at 30 °C and then switched to 37 °C overnight for double crossover (DCO). When DCO is successful, the *emr* and wild-type genes are lost. For such screening, the colonies were picked and replated on THY-agar and erythromycin/THY-agar simultaneously. The colonies that grew in THY, but not erythromycin/THY, were selected and evaluated by PCR. Successful DCO clones were also resistant to 2 μ M chloramphenicol. Confirmation of the loss of the particular gene after DCO was made through use of null PCR results with gene-specific primers (Table 1).

In addition to the above gene-deleted mutants, GAS strains with targeted mutations in specific genes (e.g. NS931/*covS*^M) were also generated. Instead of *cat* gene, the desired mutations of the gene of interest were first constructed by mutagenesis of the gene in the above targeting vectors. The SCO/DCO strategy was as described above.

Reverse Complementation of Genes—A DNA fragment comprising the entire gene of interest, along with 300–400 bp of 5' and 3' genomic flanking regions, was isolated by PCR. SacI and EcoRI restriction sites were incorporated by PCR into the 5' and 3' ends, respectively, of the fragment for ligation into the shuttle vector pDCem. The plasmid was then transformed into the GAS strain with the specific WT gene deleted and screened

for *emr*. Positive colonies were tested for gene expression by RT-PCR with gene-specific primers (supplemental Table 1).

RNA Preparation—To prepare RNA, cells at the desired growth phase were centrifuged and resuspended in 200 μ l of spheroplasting buffer (20 mM Tris-HCl, pH 6.8, 10 mM MgCl₂, 26% raffinose), containing 100 μ g/ml chloramphenicol and streptomycin. After adding 10 units of mutanolysin, the cells were pelleted and resuspended in RLT cell lysis buffer (Qiagen, Valencia, CA), and the isolation continued as described in the Qiagen RNeasy mini-kit. DNA contamination was further removed with two treatments of 4 units of DNase I (Qiagen).

Q-RT-PCR—Three independent extractions of total RNA from each of the strains were used. Real time reverse transcription-PCRs (RT-PCR) were performed essentially as described previously (23) with the primers of supplemental Table 1. The relative gene expression levels were analyzed by the $2^{-\Delta\Delta C_T}$ method (24), in which C_T represents the threshold cycle number of RT-PCR at which the amplified product was first detected. The statistical means of triplicate C_T values were calculated for the target and reference genes (in this case, *gapdh*) from both WT and mutant strains. ΔC_T was determined by C_T of target gene $- C_T$ of reference gene, and then $\Delta\Delta C_T$ was calculated by ΔC_T of mutant $- \Delta C_T$ of WT. The relative changes of a gene of interest (%) were calculated with the following equation: $100 \times 2^{-\Delta\Delta C_T}$. We employed both *gapdh* (*plr*) and *mutS* as housekeeping genes. Although *gapdh* is normally used for this purpose, its translated product is a functional protein (Plr) in this system, and thus, we confirmed all relative expression data with a second loading gene *mutS* (25).

Western Blotting—Mid-log phase GAS cell suspensions ($A_{600\text{ nm}} \sim 0.6$) were centrifuged, washed with PBS, and resuspended in PBS to $A_{600\text{ nm}} \sim 1.0$. After treating with 100 units of mutanolysin, 10% SDS was added to lyse the cells. SDS-PAGE was performed, and the proteins were transferred to PVDF membranes. These membranes were then incubated with rabbit anti-streptococcal enolase (SEn) or rabbit anti-PLR (26), followed by incubation with alkaline phosphatase-conjugated goat anti-rabbit IgG. The protein was visualized using 5-bromo-4-chloro-3-indolyl phosphate/nitro blue tetrazolium detection.

Cloning and Expression of Proteins—Full-length *sk* was cloned from the gDNAs of WT-AP53 and WT-NS931 and expressed in *Escherichia coli* cells, as reported previously (27). Recombinant (r) hPg was expressed in *Drosophila* Schneider S2 cells as described (28).

Binding of hPg to GAS Cells by ELISA—GAS cells were grown to $A_{600\text{ nm}} \sim 0.6$ and collected by centrifugation. The cells were washed and resuspended in PBS to $A_{600\text{ nm}} \sim 1.0$. A volume of 50 μ l of cell suspension containing 2×10^7 cfu of cells was used to coat individual wells of 96-well NUNC Maxisorb plates (NUNC Thermo, Rochester, NY). After blocking with 200 μ l of 1% BSA, 20 μ g/ml human nonimmune IgG, and washing with PBS, 100 μ l of 20 μ g/ml hPg in PBS was individually added. Mouse anti-hPg (ERL, South Bend, IN) in BSA blocking buffer was added, followed by horseradish peroxidase (HRP)-labeled goat anti-rabbit IgG. TMB substrate (R&D Systems, Minneapolis, MN) was used for detection at 450 nm after termination of the reaction with an equal volume of 2 M H₂SO₄. Negative con-

trols were accomplished by this same procedure with PBS in place of cells.

Binding of hPg to GAS Cells Using Flow Cytometry—GAS cells were grown at 37 °C to an $A_{600\text{ nm}} \sim 0.6$. A 20-ml aliquot of the cells was centrifuged, washed, and resuspended to $\sim 5 \times 10^7$ cfu/ml in 5 ml of PBS, 1% BSA for blocking. Aliquots (200 μ l) of cell suspensions were centrifuged, resuspended in 20 μ g/ml hPg in PBS/1% BSA, and incubated for 1 h at room temperature. The cells were then washed with PBS, incubated with mouse anti-hPg (ERL) in PBS, 1% BSA for 30 min at room temperature, washed with PBS, and incubated with AlexaFluor488 goat anti-mouse IgG (Molecular Probes, Invitrogen) in PBS, 1% BSA for 30 min at room temperature. Finally, the cells were washed and resuspended in 200 μ l of PBS, 1% paraformaldehyde for flow cytometric analysis (FCA).

FCA was conducted with a FACSAriaIII (BD Biosciences) using the 488-nm laser. Acquisition and analysis were performed by gating on side scatter (SSC-H) and fluorescence (FITC-A), setting the scales to logarithmic amplification. Cells in suspension were analyzed at a flow rate of 10 μ l/min, and 10,000 events were recorded for analysis. Each histogram was analyzed using FCS Express Version 4 software (De Novo Software, Los Angeles, CA), which provided the Median, a statistical tool that was employed to calculate the events accepted by the gating formula that fall within the specified marker. This was used to calculate the % comparative binding of hPg, relative to WT-AP53 strain, arbitrarily set at 100%. The data were plotted using GraphPad PRISM 6 software.

Activation of hPg on Bacterial Cells—Cells of each strain were grown individually in THY medium to $A_{600\text{ nm}} \sim 0.6$ and collected by centrifugation (5,000 rpm, 10 min). The cells were washed with 10 mM Hepes, 150 mM NaCl, pH 7.4, followed by resuspension in the same buffer to $A_{600\text{ nm}} \sim 1.0$.

For hPg activation assays, 20 μ l ($\sim 1 \times 10^7$ cfu) of cells was added to individual wells of a 96-well Corning NBS nonbinding microwell plate, followed by 180 μ l of 0.22 μ M hPg, 0.28 mM S2251 (H-D-Val-Leu-Lys-*p*-nitroanilide; Chromogenix, Milan, Italy) in the same buffer. Finally, 5 nM r-SK was added. The $A_{600\text{ nm}}$, which represents S2251 hydrolysis by the generated hPm, was continually measured at 30-s intervals using a plate reader.

SpeB Activity Assay—SpeB activity was measured as described (29) with overnight stationary phase cell-free culture supernatants ($A_{600\text{ nm}} \sim 1.0-1.2$). A volume of 50 μ l of the filtered supernatants was incubated with 50 μ l of the SpeB activation buffer (1 mM EDTA, 10 mM DTT, 0.1 M NaOAc, pH 5.0) for 30 min at 37 °C. Next, an equal volume of 0.6 mM *N*-benzoyl-proline-phenylalanine-arginine-*p*-nitroanilide hydrochloride (Sigma) in 0.1 M phosphate buffer, pH 7.4, was then added to the activated culture supernatant. After 1 h 30 min at 37 °C, the $A_{405\text{ nm}}$ was determined. All assays were performed in triplicate. Protein preparations were tested at least twice. Parallel assays were performed with addition of 10 μ M of cysteine protease inhibitor E64 (Sigma) to confirm the specificity (30).

Hyaluronic Acid Capsule Assays—Overnight GAS cultures ($A_{600\text{ nm}} \sim 1.0-1.2$) in THY medium were inoculated into fresh THY and grown to the mid-log phase ($A_{600\text{ nm}} \sim 0.6$). The cells were then centrifuged and resuspended in H₂O (0.5 ml). The

Inactivating Mutation in *CovS* Component of *CovRS* Operon

capsule was liberated by shaking with CHCl_3 (1 ml). The hyaluronic acid (HA) content in the aqueous phase was determined by the $A_{640 \text{ nm}}$ after addition of an equal volume of Stains-All solution (20 mg of 1-ethyl-2-[3-(1-ethylnaphtho[1,2-*d*]thiazolin-2-ylidene)-2-methylpropenyl]naphtho-[1,2-*d*]thiazolium bromide (Sigma)), 60 ml of HOAc, 100 ml of 50% formamide, as detailed previously (31). Standard curves were constructed using known concentrations of commercial HA (Sigma).

SK Assays in Washed Cell Culture Supernatants—Single colonies from plates of WT or mutant GAS strains were transferred to 2 ml of THY media and grown overnight at 37 °C. The cells were collected and washed two times with fresh THY media and resuspended in this same medium. Next, 1 ml of an overnight culture was inoculated into 35 ml of pre-warmed THY media, and the cultures were grown at 37 °C to $A_{600 \text{ nm}} \sim 0.6$ in the presence of 28 μM aSpeB inhibitor, E64 (Sigma). The cultures were centrifuged at 10,000 rpm for 20 min to remove cells, and 10 ml of supernatants were collected. This supernatant was concentrated 20 \times using 10,000 nominal molecular weight limit membrane centrifugation filters. Supernatants were washed four times with 0.1 M phosphate buffer, pH 7.2, to remove media components. To measure SK activity in these GAS culture supernatants, hPg activation assays were performed in 10 mM HEPES, pH 7.4, at 25 °C, using 0.25 mM S2251 substrate (Diapharma, West Chester, OH). The assay contained 150 mM NaCl, 0.2 μM Glu¹-hPg, 0.2 μM PAM, and 0.25 mM S2251. The reaction was accelerated by adding 10 μl of cell supernatants. The $A_{405 \text{ nm}}$ was measured at 1-min intervals for 2 h. Control reactions were performed in the absence of hPg to ensure that the proteolytic activity of supernatants was due to hPm.

Mouse Survival Studies—C57Bl/6 male mice containing the hPg transgene (32), at 6–10 weeks of age, along with WT controls, were employed for survival studies. On the day prior to injection with bacteria, depilatory cream was used to remove hair from the right rear flank of the mouse. Mice were anesthetized with isoflurane and injected subcutaneously in the right flank with $4\text{--}6 \times 10^8$ GAS cells/mouse. Mice were observed twice daily for survival up to 10 days.

RESULTS

The *mga* Regulatory Regions of GAS Strains AP53 and NS931—Sequencing began with completing the full DNA sequence of the AP53-*pam* gene using information from its partial sequence (33) and employing a strategy described earlier for generally identifying gene loci (34). The published partial DNA sequence of *pam* (GenBankTM accession number Z22219.1) was used to design internal primers, and HindIII restriction sites were used for the self-circularization of genomic DNA with T4 DNA ligase. Forward and reverse primers internal to known sequences within *pam* allowed amplification of fragments from these internal primers through

upstream 5' and downstream 3' unknown sequences. From sequence data obtained with amplicons from these primers, the ATG and TAA start and stop codons for *pam* were located, thus completing its gene sequence with codons for 12 amino acids, including the start site at the N terminus, and 31 amino acids at the C terminus, along with flanking sequences at each end.

This expanded sequence information of *pam*, along with the complete genomic sequence data of other *S. pyogenes* strains in the GenBankTM database, allowed primers to be designed to identify genes flanking *pam*. When these amplifications were successful, the clones were sequenced, and this information was used in BLAST searches to assign genes. The new sequences obtained allowed continuation of this approach to ultimately obtain the entire sequence and gene identification of the virulence region of GAS strain AP53.

The 13.4-kb DNA sequence of overlapping genomic clones revealed eight potential structural genes downstream of the stand-alone transcriptional regulator, *mga* (35), that sequentially translate to proteins with homology to IgG-binding proteins (FcR) (4), hPg-binding proteins (PAM), IgA-binding proteins (Enn) (4), a serine protease that inactivates C5a (ScpA) (5), fibronectin-binding proteins (Fbp) (36), and laminin-binding proteins (Lbp) (30), all of which play potential roles in GAS virulence. From 5' to 3', these genes are *mga-fcR-pam-enn-scpA-fbp-lbp* (Fig. 1A). The identities of these genes have been identified by homologies with previous genomic sequence results in GenBankTM, by Shine-Dalgarno sequences proximal to a translation initiation codon (supplemental Table 2), by translation stop regions, and by –35 and –10 transcription initiation sites in the 5'-proximal promoters of these putative genes. However, the AP53-*fcR* gene cannot be fully translated in this GAS strain because a single base mutation in the position corresponding to amino acid 85 of *fcR* placed a translation stop signal (TAA) at that location, in an otherwise complete gene. Similar PCR amplifications of the *fcR* gene in numerous other GAS strains did not show this stop codon.

The gene components of the proximal *mga* regulon of GAS strain NS931 have been compared with those of AP53. Although we did not completely sequence all of these genes in NS931 gDNA (full sequences have been accomplished for *mga* and *emm* and partial sequences for the remainder of the NS931 genes), we show, by using the PCR primers of supplemental Table 1, that gDNA amplicons for *mga-fcR-emm-enn-scpA-fbp-lbp* were sequentially arranged in this same order in NS931 cells and display approximately the same molecular sizes as the AP53 genes (Fig. 1B). Importantly, a different M-protein gene (*emm*) in strain NS931 replaces *pam* of strain AP53 in this same locus and does not contain the hPg-binding site that is present in PAM_{AP53}, as our translated protein sequence data shown in Sequence 1.

```
PAMAP53 90LQGLKD--DVEKLTADAELQRLKNERHEEAELERLKSERHD-
EmmNS931 89LDKKNK-----KLDSQVDGLIGVVESDEE-----
```

SEQUENCE 1

Inactivating Mutation in *CovS* Component of *CovRS* Operon

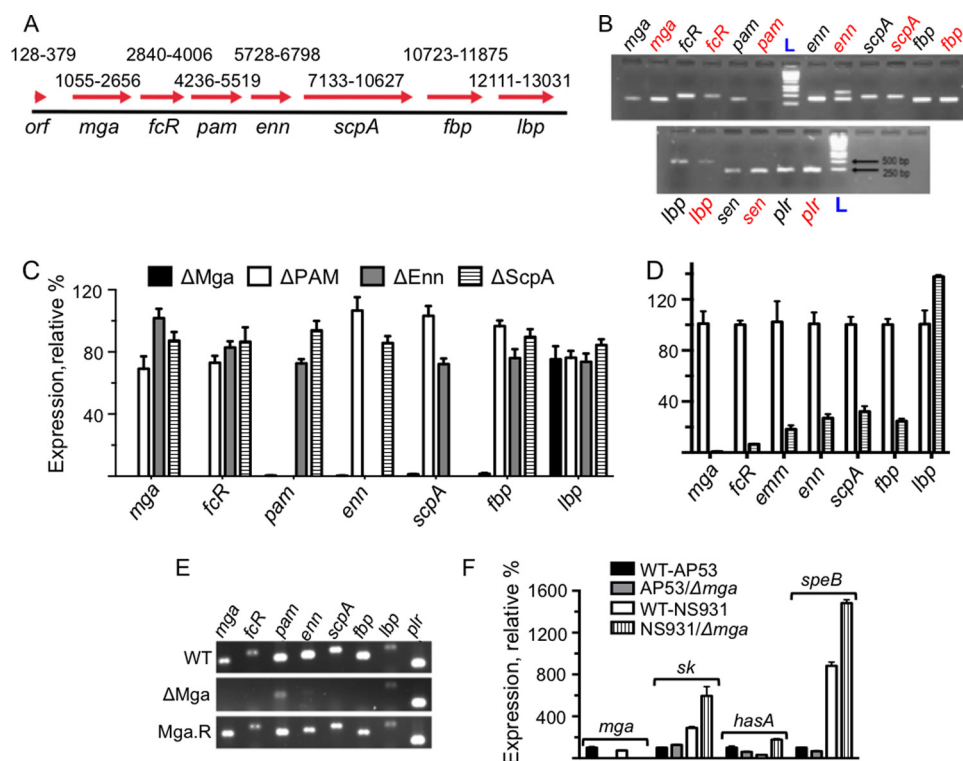


FIGURE 1. Gene arrangement and expression within the *mga* regulon region of GAS strains AP53 and NS931. *A*, total of 13,383 bp from the WT-AP53 genome was sequenced from a genomic clone (*black bar*; 1–13,383). The *red arrows* show the genes identified, their directions from 5' to 3', and their sequence positions (beginning at the ATG initiation codon to the end of the translation stop codon), arbitrarily starting at position 1 of the assembled genomic clone. The numbering *above* each *arrow* shows the range of bp from its translation initiation codon to the translation stop codon. *orf* is the open reading frame of the most 5' gene with unknown function; *mga* is the trans-acting positive regulatory gene for this core group of virulence proteins; *fcR*, which in the AP53 strain and GAS strain has a stop codon after amino acid 84 from the translation initiation site in an otherwise complete *fcR* gene, is the antiphagocytic IgG receptor gene; *pam* refers to the direct Pg-binding gene; downstream of *pam* is the *enn* gene, encoding an IgA-binding protein; which is sequentially followed by genes encoding C5a peptidase (*scpA*), fibronectin-binding protein (*fbp*), and laminin-binding protein (*lbp*). Subclones generated by PCR from homologous sequences found in other GAS strains were used to obtain overlapping gene and flanking sequences in order that the genes in the entire genomic clone were identified and positioned. *B*, PCR amplicons of individual genes in gDNA of WT-AP53 (*black*) and WT-NS931 (*red*) gDNA using the PCR primers (*supplemental Table 1*) for WT-AP53 gene sequences in *A*. The *pam* gene is not observed in NS931 cells. *C*, Q-RT-PCR analysis of the relative transcript levels of the *mga* core regulon genes in total mRNA isolated from AP53/ Δ *Mga* cells (*black bars*), AP53/ Δ PAM (*white bars*), AP53/ Δ Enn (*gray bars*), and AP53/ Δ ScpA (*striped bars*), based on each gene of WT-AP53 arbitrarily set at 100% (not shown in the figure). The WT-AP53 data were first normalized to the *gapdh* transcript level or that of a second housekeeping gene, *mutS*, in the individual total mRNA. No significant differences were found whether *gapdh* or *mutS* was used for this purpose. *D*, Q-RT-PCR analysis of the relative transcript levels of the *mga* regulon genes in total mRNA isolated from WT-NS931 cells (*white bars*) and NS931/ Δ *Mga* cells (*striped bars*), based on each gene of WT-NS931 arbitrarily set at 100%, as normalized to the *gapdh* transcript level in the individual total mRNA. The same primers for each gene were used in each WT and isogenic strains. Specific primers for the *emm* gene were used in this case. *E*, RT-PCR amplicons for *mga*, *fcR*, *pam*, *enn*, *scpA*, *fbp*, *lbp*, and *plr* (*gapdh*) examined in the isogenic strains, WT-AP53, AP53/ Δ *Mga*, and AP53/*Mga.R*. *F*, effect of inactivation of the *mga* gene on critical virulence genes outside of the *mga* core regulon in WT-AP53 and WT-NS931 cells. The % expression of the specific transcripts in total mRNA is relative to each gene set at 100% in WT-AP53 cells. Primers for individual genes between AP53 and NS931 strains were exact matches to the respective gene sequences. Data are shown for mRNA of *sk*, the *hasA* component of the *hasABC* regulon, and the cysteine protease *speB*.

The *a1*(*italics*)/*a2*(**boldface**) locus, which contains the hPg-binding site in PAM_{AP53} (amino acids sufficient and critical for hPg binding are underlined) (19, 37–39), is not present in EMM_{NS931}, thus rendering this M-protein incapable of directly binding to hPg.

Transcription of Genes within the Core *mga* Regulon—RT-PCR analysis of the isolated mRNA amplicons from this isogenic AP53 strain with gene-specific primers (*supplemental Table 1*) demonstrated that *fcR*, *pam/emm*, *enn*, *scpA*, and *fbp* were severely down-regulated in mRNA from log phase ($A_{600\text{ nm}} \sim 0.6$) cultures of AP53/ Δ *mga* (Fig. 1C) and NS931/ Δ *mga* (Fig. 1D), as compared with their respective WT strains. The mRNA level of *lbp* was not significantly altered by the *mga* deletion in either strain (Fig. 1, C and D). In addition, deletions of genes for *pam*, *enn*, and *scpA* did not influence genes of any other *Mga* core regulon genes (Fig. 1C). For these experiments, we arbitrarily set the relative expression of each tested gene of

WT-AP53 and WT-NS931 at 100%, because our interest here was to only compare the effect of a *mga* gene inactivation on the expression of individual genes in each strain. Loading controls were accomplished with *gapdh* and *mutS*, with the results unaffected by the nature of the housekeeping gene used.

The data from Fig. 1, C and D, show that the boundaries of the *mga* core regulon in both AP53 and NS931 strains are 5'-*mga*-through-*fbp*-3'. The down-regulation of genes for *fcR*, *pam*, *enn*, *scpA*, and *fbp* seen in strain AP53/ Δ *mga* was reversed in the mutant bacterial strain that was reverse-complemented with the WT-*mga* gene yielding AP53/*mga.R* (Fig. 1E). This recomplemented cell line was shown by Q-RT-PCR to produce 118% of *mga* and 115% of *pam*, compared with these transcripts in WT-AP53, taken as 100%. Thus, both WT-AP53 and WT-NS931 GAS strains contain the large *vir* (*mga*) core regulon (40), with identical components except for the nature of the M-protein.

Inactivating Mutation in *CovS* Component of *CovRS* Operon

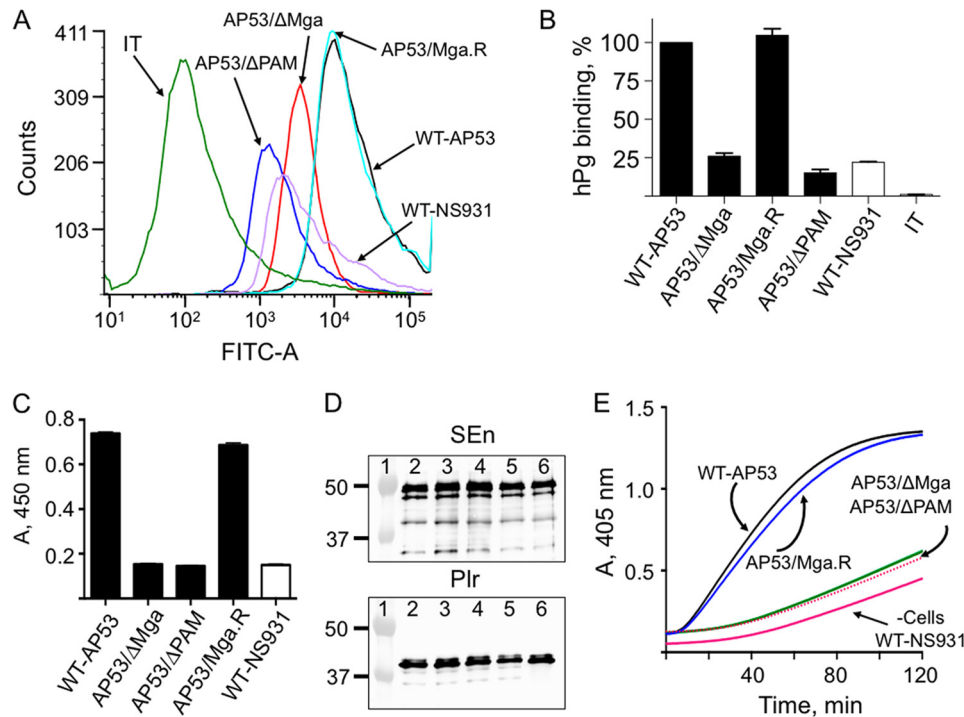


FIGURE 2. Binding and activation of hPg to GAS cells. *A*, binding of hPg to the indicated strains of GAS was examined by FCA. Cells of each GAS line (1×10^7 cfu) were incubated with hPg (20 μ g/ml). Mouse anti-human Pg was added, followed by AlexaFluor488 goat anti-mouse IgG. The cells were then resuspended in PBS, 1% paraformaldehyde for FCA. FCA histograms for each of the cell lines are shown at 488 nm, with gating on side scatter (SSC-H) and fluorescence (FITC-A), using logarithmic amplification. The cell suspensions were analyzed at a flow rate of 10 μ l/min with 10,000 events used for analysis. *IT* represents the antibody isotype control. *B*, % binding of hPg calculated from *A*. The hPg binding to WT-AP53 was taken as 100%; the binding by other strains was calculated using the Median statistical value provided from analysis of each FCA histogram by FCS Express version 4 software. *C*, hPg binding measured by ELISA. Cells ($\sim 2 \times 10^7$ cfu) from log phase growth ($A_{600\text{ nm}} \sim 0.6$) of the indicated strains of GAS were added to individual wells of 96-well microtiter plates. Next, hPg was added, followed sequentially by rabbit anti-human Pg and HRP-conjugated goat anti-rabbit IgG, with washes between additions. After addition of the HRP substrate TMB, for 20 min, the reaction was terminated with 2 M H_2SO_4 , and the $A_{405\text{ nm}}$ was determined and plotted directly. *D*, SEn and Plr expression detected by Western blot analysis of whole cell extracts of each cell line. The $A_{280\text{ nm}}$ was adjusted to 0.3, and 10 μ l was applied to each lane. The antibodies employed were anti-SEn (top) and anti-Plr (bottom). Lane 1, molecular weight markers; lane 2, WT-AP53; lane 3, AP53/ΔPAM; lane 4, AP53/ΔMga; lane 5, AP53/Mga.R; lane 6, WT-NS931. *E*, cells of the GAS strains indicated were grown to $A_{600\text{ nm}} \sim 0.6$ in 10 mM Hepes, 150 mM NaCl, pH 7.0. Aliquots of cells (1×10^7 cfu) were added to individual wells of 96-well low protein binding microtiter plates. hPg was then added followed by a solution containing 5 nM r-SK2b/0.25 mM S-2251. The $A_{405\text{ nm}}$ was continuously monitored using a plate reader. The data were collected at room temperature. The red line, represented as -Cells, is a control activation in the absence of cells and is very similar to the activation rate seen with WT-NS931 cells. There was no difference in the curves when E64 was placed in the cell growth medium and the assay.

Genes outside of this core *mga* regulon are controlled directly or indirectly by Mga. Specifically, we examined the influence of Mga on three critical virulence genes of interest to this work, *viz.* the hPg activator, streptokinase (*sk*), *hasA*, the first gene of the hyaluronate synthetase operon that provides the bacterial capsule, and *speB*, a gene that encodes a bacterial cysteine protease that can degrade SK, as well as other bacterial surface virulence-resistance genes, *e.g.* PAM. Minimal effects (≤ 2 -fold) of an *mga* gene inactivation were observed on transcript levels of *sk*, *hasA*, and *speB*, when compared with their parent AP53 and NS931 cells (Fig. 1*F*). In Fig. 1*F*, the relative expression of each gene in WT-AP53 cells was set at 100%, because we wished to obtain a general idea of gene-specific expression levels between strains, a valid approach for this gene set because the primer sequences used for amplification of these genes were exact matches between strains AP53 and NS931.

Binding of hPg to GAS Cells—Using FCA (Fig. 2, *A* and *B*), as well as a sandwich ELISA with in-house antibodies against hPg (Fig. 2*C*), we show that mid-log phase cultures ($A_{600\text{ nm}} \sim 0.6$) of WT-AP53 bind hPg. Under these same conditions, WT-NS931, AP53/Δ*mga*, and AP53/Δ*pam* show a reduction of ~ 80 – 90%

in hPg binding, undoubtedly because of the absence, inactivation, and/or down-regulation of PAM expression in these cell lines. When AP53/Mga.R cells were examined in this regard, binding of hPg was very similar to WT-AP53 (Fig. 2, *A*–*C*). This suggests that other hPg receptors and/or hPg-binding proteins, *e.g.* SEn and Plr, which are expressed similarly in each of these cell lines (Fig. 2*D*), are relatively less important than PAM as cellular hPg receptors, at least when PAM is present as the M-protein in the strains. A similar observation using another approach has been reported in another GAS strain, NS88.2, that contains a PAM-related protein (22).

Activation of hPg by r-SK2b on *S. pyogenes* Cells—We examined whether the binding of hPg to PAM on AP53 cells stimulates its activation by exogenous r-SK2b, cloned from AP53 cells. The data (Fig. 2*E*) show that the activation of hPg by r-SK2b, which is the form of SK that optimally acts on cell-bound hPg, is highly stimulated by AP53 cells. With AP53/ΔPAM, AP53/ΔMga, or WT-NS931 cells, none of which produce PAM, very little hPg is activated under these conditions by r-SK2b (Fig. 2*E*) and is similar to the control activation without cells (-Cells). The low activation capacities of these cell lines demonstrate that other hPg receptors, *e.g.* SEn and Plr on AP53

Inactivating Mutation in *CovS* Component of *CovRS* Operon

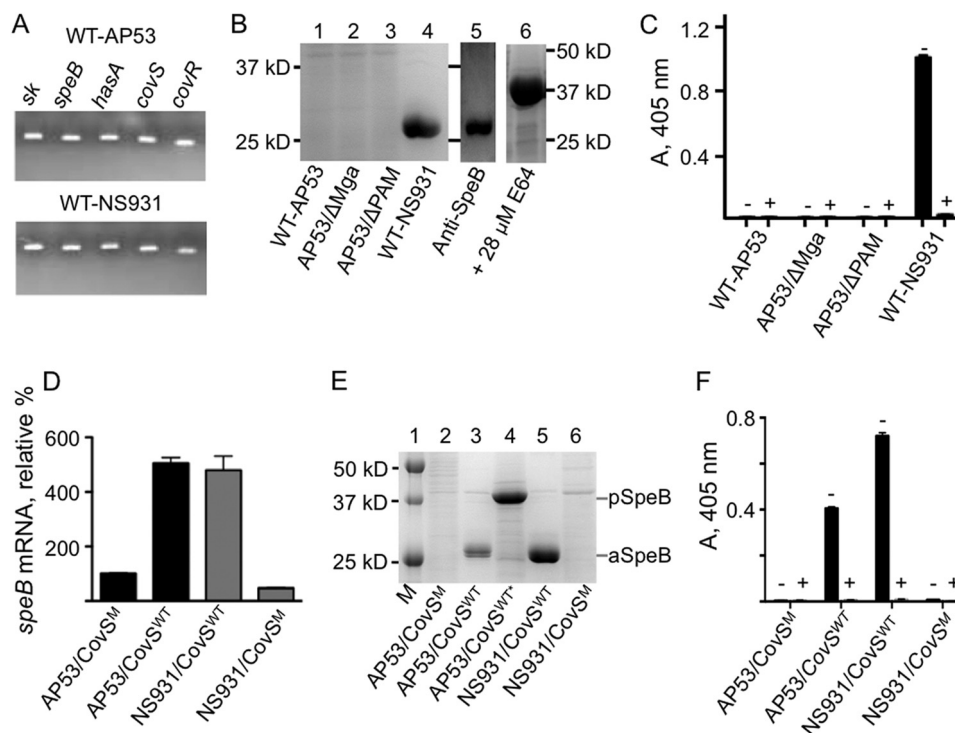


FIGURE 3. Effect of the *CovS* mutation on *CovRS* gene regulation. *A*, PCR using RT-PCR primers (supplemental Table 1) showing gDNA amplicons of some typical genes in WT-AP53 and WT-NS931 strains that are typically regulated by *CovRS*. *B*, SDS-PAGE of late-log phase ($A_{600\text{ nm}} \sim 1.0$) GAS culture supernatants in the absence of E64. Lane 1, WT-AP53 (AP53/*CovS*^M); lane 2, AP53/ Δ Mga (AP53/*CovS*^M/ Δ Mga); lane 3, AP53/ Δ PAM (AP53/*CovS*^M/ Δ PAM); lane 4, WT-NS931 (NS931/*CovS*^{WT}); lane 5, a blot of the WT-NS931 culture supernatant of lane 4 with commercial anti-SpeB; lane 6, a gel of the culture supernatant of WT-NS931 cells, grown in the presence of 28 μ M of the SpeB inhibitor E64. Gels 5 and 6 were run at different times from each other and from the gels of lanes 1–4. The molecular mass of activated mature SpeB (aSpeB) is $\sim 28,000$ and that of SpeB zymogen (pSpeB) is $\sim 39,000$. *C*, aSpeB enzymatic activity, using the substrate benzoyl-proline-phenylalanine-arginine-*p*-nitroanilide-HCl of late-LP ($A_{600\text{ nm}} \sim 1.0$) GAS culture supernatants of the indicated cell lines in the absence (–) of E64 and in the presence (+) of 28 μ M E64. *D–F*, restoration of *CovRS* system in AP53 cells. *D*, Q-RT-PCR measurements displaying relative levels of *speB* transcripts in late-log phase ($A_{600\text{ nm}} \sim 1.0$) GAS cell total mRNA, relative to WT-AP53 (AP53/*CovS*^M), arbitrarily set at 100%. *E*, SDS-PAGE of the late-log phase ($A_{600\text{ nm}} \sim 1.0$) cell culture supernatants of the following: lane 1, molecular weight markers (*M*); lane 2, AP53/*CovS*^M (WT-AP53); lane 3, AP53/*CovS*^{WT}; lane 4, AP53/*CovS*^{WT}*, except that the cells represented in lane 3 were grown in the presence of the SpeB inhibitor E64; lane 5, NS931/*CovS*^{WT} (WT-NS931); lane 6, NS931/*CovS*^M. *F*, aSpeB enzymatic activity at late-log phase ($A_{600\text{ nm}} \sim 1.0$) growth of whole cell extracts of the indicated cell lines toward the aSpeB substrate, benzoyl-proline-phenylalanine-arginine-*p*-nitroanilide-HCl, in the absence (–) and presence (+) of the aSpeB inhibitor, E64.

cells (Fig. 2*D*), do not stimulate hPg activation by SK2b to nearly the same extent as PAM. The isogenic strain, AP53/Mga.R, which elevates the highly diminished PAM levels of AP53/ Δ Mga cells to WT-AP53 levels, also restores the activation rates of hPg by SK2b to those of WT-AP53 cells (Fig. 2*E*). Thus, SK2b-producing invasive GAS strains require PAM or a PAM-like analog for optimal activation of hPg.

***CovRS* Regulatory System in AP53 Cells**—The two-component *CovRS* gene regulatory system, the genes of which are consecutively present on all GAS genomes studied, including WT-AP53 and WT-NS931 cells (Fig. 3*A*), was examined. The *covRS* operon, controlled by a single promoter upstream of *covR* (41), has been recently linked to positive regulation of the *mga*

gene, via *rivRX* (23). If this is the case, the expression of *pam* mRNA should also be indirectly regulated by *covRS*. To examine this point, we first sought to evaluate the integrity of the *covRS* system in WT-AP53 and WT-NS931 cells that originated from GAS isolates. Full genomic sequences of the entire *covRS* bicistronic locus from these AP53 and NS931 strains yielded >99% identical WT-*covR* sequences, compared with each other and to *covR* from numerous GAS strains in the GenBank™ database, and also contained an intact WT-*covS* gene in WT-NS931 DNA. However, *covS* from AP53 DNA showed a deletion of Thr¹⁴⁰⁴ (numbered from ATG of *covS*), resulting in the following translated *CovS* protein sequence differences shown in Sequence 2.

NS931-*CovS*^{1–458 459}GIGLSILKQ⁴⁶⁷IVDGYHLQMKVESELNEGSVFIHLIPLAQSKE⁵⁰⁰
 *AP53-*CovS*^{1–458459}GIGLSILKQ⁴⁶⁷*

SEQUENCE 2

Effect of the Truncation Mutant of *CovS* (*CovS*^M) on Function of *CovRS*—To determine whether this particular mutation in *CovS* affected its ability to regulate *CovR*, we examined several

of the genes that are known to be regulated by the *CovRS* system, e.g. *speB*, *hasA*, and *sk*. Many of these essential genes exist in both AP53 and NS931, as seen by the presence of predicted

Inactivating Mutation in CovS Component of CovRS Operon

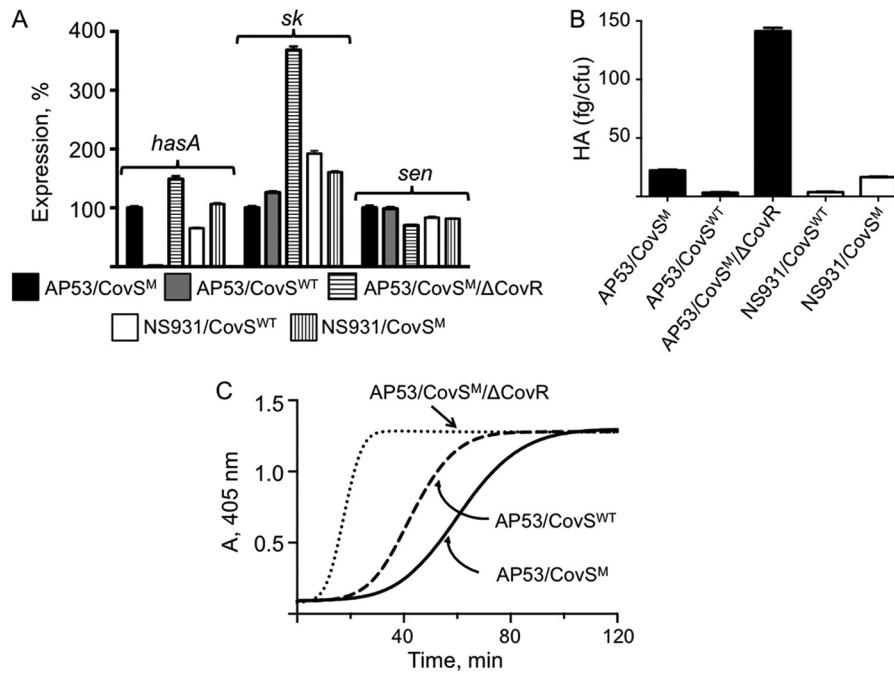


FIGURE 4. Regulation of virulence genes by CovRS in GAS. *A*, effect of the inactivation of CovS (CovS^M) and CovR (ΔCovR) on the transcription levels of *hasA*, *sk*, and *sen* genes. The levels of each specific transcript in the total mRNA of the indicated cell lines, relative to expression of each of the genes in AP53/CovS^{WT} (WT-AP53) cells arbitrarily set at 100%, are shown. Both *gapdh* and *mutS* were used as loading controls, with the results of *A* not differing with either housekeeping gene. *B*, amount of HA-containing capsule in AP53/CovS^M (WT-AP53), AP53/CovS^{WT}, AP53/CovS^M/ΔCovR, NS931/CovS^{WT} (WT-NS931), and NS931/CovS^M. *C*, activation of hPg by mid-log phase culture supernatants ($A_{600\text{ nm}} \sim 0.6$) of the cell lines indicated on the graph.

gDNA amplicons generated with specific primers for these genes (Fig. 3A).

The gene encoding the cysteine protease, *speB*, is present in all GAS strains investigated and is known to be highly up-regulated by WT-CovRS. CovR represses transcription of *speB* (42), whereas CovRS enhances transcription of this gene (43). The zymogen form of SpeB (pSpeB), of $M_r \sim 40,000$, is produced in the late-LP of GAS cell growth and is proteolytically cleaved to the active form of SpeB (aSpeB), of $M_r \sim 28,000$ (30, 44). The protein gels of concentrated culture supernatants of late-LP GAS cells ($A_{600\text{ nm}} \sim 1.0$) (Fig. 3B) do not show evidence for SpeB in either AP53/CovS^M (WT-AP53) or its WT isogenic mutants, AP53/ΔMga, AP53/CovS^M/ΔMga (AP53/ΔMga), and AP53/CovS^M/ΔMga (AP53/ΔPAM) (lanes 1–3), likely due to repression by CovR that is not controlled by the CovS mutant found in WT-AP53 cells. However, WT-NS931 cells (NS931/CovS^{WT}), containing WT-CovS, produce comparatively large amounts of protein of the appropriate size of aSpeB (Fig. 3B, lane 4), which reacts with anti-SpeB (lane 5). When WT-NS931 cells are grown in the presence of the aSpeB inhibitor E64, only pSpeB is produced (Fig. 3B, lane 6). These results are confirmed in enzymatic assays of these late-LP culture supernatants (Fig. 3C), wherein no aSpeB activity toward the substrate, benzoyl-proline-phenylalanine-arginine-*p*-nitroanilide-HCl, is seen in culture supernatants from AP53 cells and its indicated isogenic variants. However, high aSpeB activity is observed in late LP supernatants from NS931 cells in the absence of the aSpeB inhibitor E64 (–) but not in the presence (+) of this inhibitor.

The effect of the natural CovS mutation found in WT-AP53 cells on SpeB expression has been examined (Fig. 3, D–F). Q-RT-PCR of total cell mRNA, using specific *speB* primers

(supplemental Table 1), shows that total mRNA of AP53 cells with the natural truncation mutant corrected to that of CovS^{WT} (AP53/CovS^{WT}) produces ~ 5 times more *speB* transcript than that contained in total mRNA from AP53/CovS^M cells. Similarly, total mRNA from NS931/CovS^{WT} cells expresses ~ 8 times higher levels of the mRNA for *speB* than the total mRNA from NS931/CovS^M cells. The SDS-PAGE protein gel data (Fig. 3E) are in agreement with this conclusion. Here, late-LP culture supernatants of the mutated cell line, AP53/CovS^{WT} (Fig. 3E, lane 3), produce much more aSpeB than culture supernatants from WT-AP53 cells (lane 2), whereas the converse is true in WT-NS931 (lane 5) and NS931/CovS^M (lane 6) cells. Growth of AP53/CovS^{WT} cells in the presence of 28 μM E64 (Fig. 3E, lane 4), as with growth of WT-NS931 cells under these same conditions (Fig. 3B, lane 6), produce only pSpeB. aSpeB activity assays (Fig. 3F) fully confirm these findings in that only late-LP AP53/CovS^{WT} and NS931/CovS^{WT} cell supernatants produce aSpeB, when grown in the absence (–) of E64, but not in its presence (+).

Whereas WT-CovRS stimulates *speB* expression, this system represses the *hasABC* regulon, thus potentially reducing capsule production (45). We show that under nonstress conditions CovS^{WT} is required to repress the repression of *hasA* by CovR^{WT}, a conclusion that is not in agreement with previous work (16). Specifically, the data (Fig. 4, A and B) demonstrate that the amount of *hasA* present in AP53/CovS^M (WT-AP53) cells is ~ 10 times higher in *hasA* mRNA levels (Fig. 4A) and ~ 12 -fold higher in hyaluronic acid (HA) content, when compared with its isogenic mutant cell line, AP53/CovS^{WT}. Similarly, the amount of *hasA* is ~ 2 -fold higher in NS931/CovS^M cells (Fig. 4A) and is ~ 5 -fold higher in HA (Fig. 4B) content

than in WT-NS931/*CovS*^{WT} (WT-NS931) cells (Fig. 4A). These data show that whereas WT-*CovRS* indeed represses *hasA* and HA, the dominant role is provided by *CovR*, as is seen by the dramatically increased expression of *hasA* and HA in AP53/*CovS*^M/ Δ *CovR* cells (Fig. 4, A and B).

In a similar vein, it has been shown previously that *sk* transcription is repressed by *CovR* (46), but the specific influence of *CovS* on *CovR* repression of *sk2b* regulation is more uncertain. Accordingly, we investigated the functional effect of *CovS* on SK2b production in AP53 cells through examination of the activation of hPg by dialyzed whole cell culture supernatants of mid-log phase ($A_{600\text{ nm}} \sim 0.6$) GAS cells. E64 (28 μM) was maintained in the inoculated cultures and in assays to inhibit the known degradation of SK by aSpeB (47). The data obtained show that AP53 cells mutated to display the WT-*CovRS* system, *viz.* AP53/*CovS*^{WT} cells, possess slightly higher mRNA levels of *sk* (Fig. 4A), and corresponding higher activation rates (~ 1.5 times) of hPg are seen (Fig. 4C), as compared with isogenic cells with intact *CovR* and inactive *CovS* (e.g. WT-AP53 cells). Similar small differences were observed in NS931/*CovS*^{WT} (WT-NS931) and NS931/*CovS*^M cells (data not shown). Deletion of *CovR* from WT-AP53 (AP53/*CovS*^M/ Δ *CovR*) cells shows an ~ 4 times increase in mRNA levels of *sk* (Fig. 4A) and a corresponding larger amount of SK2b protein in the supernatant (Fig. 4C). Because the overall differences in the AP53 strain made by *CovS* inactivation are small (~ 1.5 – 2 -fold), the data suggest that *CovS* plays a minor role with regard to regulation of the *sk* gene under normal cell growth conditions, and the repressor role of *CovR* on *sk* transcription and corresponding protein expression is dominant, albeit not large (3.5–4.5 times).

Interaction of the *covRS* Operon With *mga* Regulon—It has been proposed that the *CovRS* system indirectly regulates expression of the *mga* gene, through *rivRX* (23). If that is the case, indirect effects should be observed with expression of *pam*, and we have assessed the functional consequences of changes in PAM expression through binding of hPg to the various mutated cell lines and through the corresponding activation of hPg by SK2b in the presence of these same GAS strains. WT-AP53 cells have been used as the reference for comparisons of the binding of hPg to other GAS cells. Relative mRNA levels of another hPg receptor, *sen*, are not affected by *covS* or *covR* gene inactivations (Fig. 4A). The data for hPg binding to various isogenic cell lines obtained by FCA (Fig. 5, A and B) and specific ELISA (Fig. 5C) show that AP53/*CovS*^M (WT-AP53) cells and AP53/*CovS*^{WT} cells bind hPg very similarly, with only $\sim 10\%$ increased binding to AP53/*CovS*^{WT} cells. This small increase in binding is apparently not productive, because it is seen (Fig. 5D) that activation by exogenous SK2b in the presence of AP53/*CovS*^{WT} cells is even lower than this same activation in the presence of AP53/*CovS*^M cells. These assays were performed both in the absence of E64 and in the presence of 28 μM E64 to inhibit the possible degradation of SK by aSpeB and the release of PAM from the cell surface, another known activity of aSpeB. Thus, under normal laboratory growth conditions, *CovS* does not play a regulatory role on *CovR* with regard to *mga* regulation. In fact, Q-RT-PCR results (data not shown) for levels of the *mga* mRNA in total mRNA isolated from AP53/

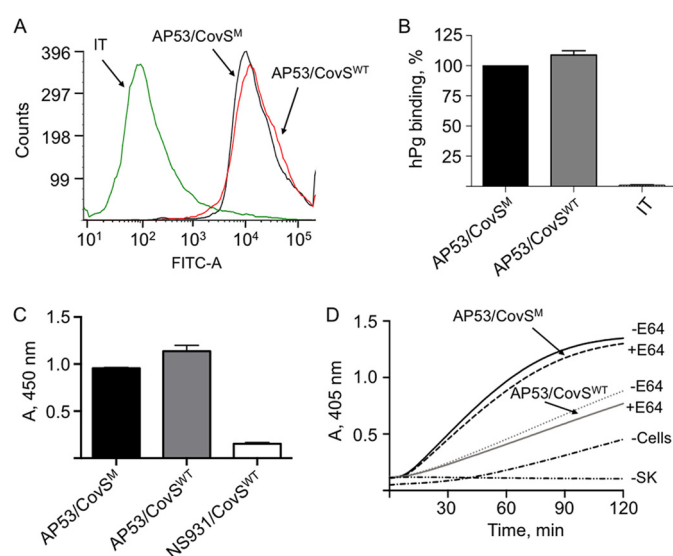


FIGURE 5. Effect of the *CovS*^M on functional expression of PAM. A, binding of hPg to AP53/*CovS*^M (WT-AP53) cells and AP53/*CovS*^{WT} cells as assessed with FCA. Cells (1×10^7 cfu) were incubated with hPg (20 $\mu\text{g}/\text{ml}$). Mouse anti-human Pg was added, followed by AlexaFluor488 goat anti-mouse IgG. The cells were then resuspended in PBS, 1% paraformaldehyde for FCA. FCA histograms for each of the cell lines are shown at 488 nm, with gating on side scatter (SSC-H) and fluorescence (FITC-A), using logarithmic amplification. The cell suspensions were analyzed at a flow rate of 1 ml/s with 10,000 events used for analysis. IT represents the antibody isotype control. B, % binding of hPg to AP53/*CovS*^{WT} cells, relative to hPg binding to AP53/*CovS*^M set at 100%, was calculated using the median statistical value provided from analysis of each FCA histogram by FCS Express version 4 software. C, cells ($\sim 2 \times 10^7$ cfu) of the indicated strains of GAS were added to individual wells of 96-well microtiter plates. Next, hPg was added, followed sequentially by rabbit anti-human Pg and then HRP-conjugated goat anti-rabbit IgG. After addition of the HRP substrate TMB for 20 min, the reaction was terminated with 2 M H_2SO_4 , and the $A_{450\text{ nm}}$ was determined. D, cells (1×10^7 cfu) were added to individual wells of 96-well low protein binding microtiter plates. hPg was then added followed by a solution containing 5 nmol r-SK2b/0.25 mM S-2251. The $A_{405\text{ nm}}$ was continuously monitored on a plate reader. The data were collected at room temperature. The lines represented as -Cells and -SK are control activations in the absence of cells and SK, respectively. All cells were presented at mid-log phase growth ($A_{600\text{ nm}} \sim 0.6$). Assays were performed both in the absence (-E64) and presence (+E64, 28 μM) of the aSpeB inhibitor, E64, in each cell line during cell growth and during the hPg activation assay.

CovS^M cells and AP53/*CovS*^{WT} cells show no significant differences.

We considered whether the *CovS*-inactivating mutation in WT-AP53 cells was a result of genetic drift of this bacterium or whether it resulted in the AP53 isolate in the patient from an *in vivo* phase shift in *CovRS* of the cells under stress. This latter phenomenon occurs in GAS and is employed by the bacteria to rapidly up- or down-regulate genes that assist its survival in the host at different stages of infection. It has been reported that in an M1T1 GAS strain, M1, the HA capsule, and/or a DNase I (*sda1*) expressed by a bacteriophage acquired by the GAS during evolution are necessary for this hyperinvasive genetic phase switching to occur (48, 49). To determine whether genotypic switching in *covRS* could occur in the AP53 GAS strain, which has M-like protein and capsule, but not Sda1, we infected mice, subcutaneously, with AP53/*CovS*^{WT} cells and reisolated the cells from the skin lesion that developed 3 days after infection. We then examined aSpeB production in the GAS colonies obtained (Fig. 6, A–C). aSpeB production would be down-regulated if *CovR* and/or *CovS* was inactivated during infection.

Inactivating Mutation in *CovS* Component of *CovRS* Operon

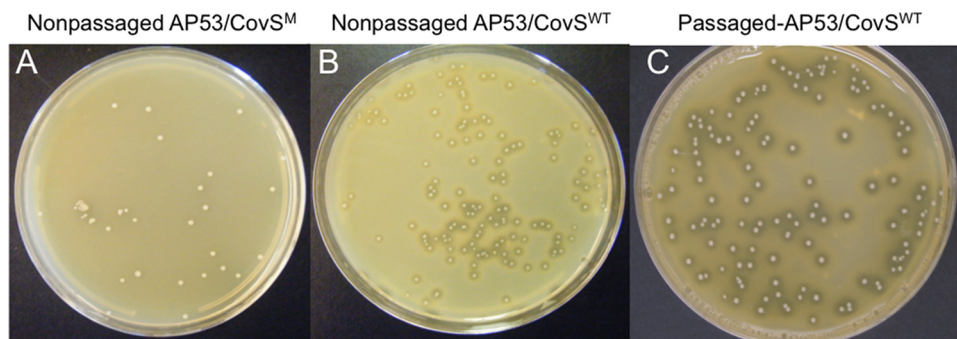


FIGURE 6. Genetic switching of *CovS* in AP53 cells. AP53/*CovS*^{WT} cells (7×10^9 cfu) were injected subcutaneously into C57Bl/6 mice. Skin lesions were harvested after 3 days and homogenized. Dilutions were plated on THY/milk medium, and production of aSpeB from individual colonies was observed by the lytic zones surrounding the cells. A total of 1,500 colonies/mouse was screened for each of three mice. The unpassaged cells were prepared similarly to the injected cells. **A**, unpassaged AP53/*CovS*^M (WT-AP53) cells. No aSpeB was observed. **B**, unpassaged AP53/*CovS*^{WT} cells. aSpeB was produced in all clones. **C**, passaged AP53/*CovS*^{WT} cells. aSpeB was produced in all clones, suggesting that *CovR/CovS* remained as WT proteins and stimulated aSpeB production.

The results obtained from screening 1,500 colonies/mouse from the active infection in each of three mice demonstrated that aSpeB was produced in all colonies, as seen by the lytic zones surrounding each single colony (Fig. 6C). That this assay would detect such a mutation in *CovR*^{WT} or *CovS*^{WT} is also demonstrated in Fig. 6. Here, noninjected AP53/*CovS*^M cells do not show lysis zones around the clones (Fig. 6A), but noninjected AP53/*CovS*^{WT} isogenic cells do show these lytic zones (Fig. 6B). In addition to these experiments, we accomplished total nucleotide sequencing of the entire *covR-covS* genomic region, amplified by RT-PCR, from five randomly chosen clones from each of three of the plates of passaged AP53/*CovS*^{WT} cells of Fig. 6C. The results demonstrated that only WT-*covRS* was present. Thus, *CovR* and *CovS* retained their WT status during infection and continued to up-regulate *speB* in AP53/*CovS*^{WT} cells during the active infection.

Finally, the effects of these variant cell lines on survival of mice containing the hPg transgene (hPg(Tg)) have been investigated. The data obtained are shown in Fig. 7. After subcutaneous administration of $\sim 5 \times 10^8$ AP53/*CovS*^M (WT-AP53) cells, 14/15 C57Bl/6(hPg(Tg)) mice expired within 5 days, and C57Bl/6 mice that did not contain hPg(Tg) survived for the full 10 days of observation (data not shown), in agreement with earlier observations (32). Deletion of the *scpA* or *enn* genes from AP53/*CovS*^M cells did not protect mice against lethality in this model; 8/8 and 6/7 of the AP53/*CovS*^M/Δ*ScpA* and AP53/*CovS*^M/Δ*Enn*, respectively, died at the same rate as AP53/*CovS*^M mice (Fig. 7A). A total of 5/9 and 4/7 AP53/*CovS*^M/Δ*PAM* and AP53/*CovS*^M/Δ*Mga* treated mice survived the entire 10 days (Fig. 7A), demonstrating the protection against lethality by deletion of these genes. Alteration of *CovS*^M in AP53/*CovS*^M cells to AP53/*CovS*^{WT} offered nearly complete protection from lethality in C57Bl/6(hPg(Tg)) mice (Fig. 7A). This result further supports the point that *CovS*^{WT} is not being mutated in the animal during the infection. These data also suggest that hPg and PAM are important for GAS lethality in this model, which also requires an intact and functional *CovRS* system. A similar trend is observed using a strain of PAM⁻ bacteria, NS931, with C57Bl/6(hPg(Tg)) mice (Fig. 7B). In this case, NS931/*CovS*^M-injected mice die at a much faster rate than mice injected with the NS931/*CovS*^{WT} strain. Although hPm is not produced by the same route with this latter bacterial strain,

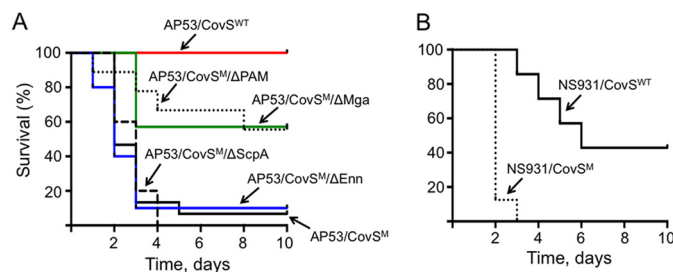


FIGURE 7. Lethality of AP53 GAS strains. GAS cells ($\sim 4-6 \times 10^9$ cfu for each GAS strain) of the indicated GAS cell lines were injected in C57Bl/6-hPg(Tg) mice ($n = 7-10$ mice for each GAS strain). Survival was monitored up to 10 days. **A**, bacterial strains isogenic with AP53/*CovS*^M (WT-AP53) cells. **B**, NS931/*CovS*^{WT} (WT-NS931) and NS931/*CovS*^M cells. The *CovS* mutant generated in this strain is the same as found in WT-AP53 cells.

it is nonetheless produced in plasma rather than the bacterial surface, because the SK1 generated by these bacteria do not require PAM for surface activation of hPg and will generate hPm in the solution state.

DISCUSSION

A 13.4-kb genomic fragment of *S. pyogenes* pattern D strain AP53, bound by the *mga* and *lbp* genes, contains sequentially *mga-fcR-pam-enn-scpA-fbp-lbp*, within which the M protein pathogenicity region of the genome is found. It has been reported that SOF⁻ strains of *S. pyogenes* rarely contain this full complement of M-protein-related genes in this DNA island and typically lack *fcR* and *enn* (50, 51). AP53, which is SOF⁻, violates this paradigm, as does NS931, which also contains this same gene pattern in the *mga*-dependent virulence region. Upon comparing 5'-promoter sequences of each of the genes with the consensus Mga-binding sequence (52), we find homologies with promoter sequences of *mga*, *fcR*, *pam*, *enn*, and *scpA* but not with 5'-proximal sequences of *fbp* and *lbp*. Although *lbp* is not regulated by Mga, as would be predicted, we show that *fbp* transcription is strongly down-regulated by an inactivation of the *mga* gene in both AP53 and NS931 strains of GAS. Thus, it is possible that *fbp* is a member of a polycistronic gene, regulated by a promoter of an upstream gene, most likely *scpA*, or is more indirectly influenced by *mga*. Thus, with the possible exception of bicistronic *scpA-fbp* transcription, all of the genes in this region are most likely monocistronic, because they independently possess proximal promoter homologies to the Mga-

binding consensus polynucleotide. As has been found in other *S. pyogenes* strains, disruption of the *mga* gene directly and indirectly affects transcription of many other genes outside of this M-protein virulence island (53).

This study expands the previous fingerprint and restriction mapping analyses of this virulence region of a number of isolates with *pam*-like genes (54–56) to an identification of its gene structure and regulation. Our interest in the AP53 bacterial strain was governed by the direct dependence of its virulence on the integrity of the human host fibrinolytic system. Cell surface acquisition of hPg is important to the virulence of this class of bacteria in humans, and in the case of GAS, hPg binding is a critical virulence determinant (10, 56). Other virulence mechanisms surely exist, and the importance of the host Pg pathway may be a property of those strains that can assemble host hPg on the surface of the bacteria via direct binding to PAM or indirect binding to the host fibrinogen that itself interacts with fibrinogen-binding M-proteins. In fact, another strain used in this report, NS931, closely resembles the gene arrangement within the *mga* regulon. This strain is also an invasive isolate from skin. It does not contain PAM, and thus functions somewhat differently. Thus, although PAM is an essential virulence factor for AP53, other strains do not require PAM and likely function at different end points of virulence as mechanisms for survival of GAS, as the host adapts.

During sequence analysis of AP53, we discovered a truncation mutation in *CovS* (*CovS^M*), the sensor constituent of the two-component *CovRS* system, that allows GAS gene expression to respond to a variety of environmental challenges by the host, such as $[Mg^{2+}]$, osmolality, temperature, etc. (16). It is likely that differences in gene regulation by the *CovRS* system (41), which both up- and down-regulates a large number of genes in the bacterial genome (57), is responsible for some of the different properties of these two GAS strains. We focused on some key virulence genes of importance to our work, *viz.* *speB*, *hasA*, *sk*, and *pam*. It is possible that this latter gene is influenced indirectly via effects of *CovRS* on the *mga* gene.

Using the important virulence factor, *speB*, the gene that encodes the cysteine proteinase precursor, pSpeB, as one model of gene up-regulation wherein WT-*CovS* derepresses *CovR* on gene expression (43), we find that *CovR* attenuates *speB* expression in GAS strains possessing the truncated *CovS* found in WT-AP53 and in the NS931 strain in which that same mutation was engineered in NS931 (NS931/*CovS^M*). However, in WT-*CovRS* systems, *e.g.* WT-NS931, and an engineered GAS strain, AP53/*CovS^{WT}*, *speB* expression is highly up-regulated. Because *CovS* does not function in the absence of *CovR*, but *CovR* can function in the absence or presence of *CovS* (43), the natural *CovS* mutation found in WT-AP53 must be considered a mechanism used by GAS to activate the repressor activity of *CovR* toward the *speB* gene. To be effective, this mode of regulation of gene expression by genetic switching also would be required to occur rapidly at different stages of an active infection, as has been found (58). Because aSpeB assists in the initial stages of infection in terms of matrix degradation, but inhibits subsequent bacterial dissemination by digesting virulence factors, *e.g.* PAM and SK, a rapid switch exists to enhance and attenuate expression of such virulence proteins. The *CovRS* system that

chemically responds to environmental changes, via *CovS*, and can directly regulate gene expression through phosphorylation/dephosphorylation of *CovR*, is such as system (59).

The opposite activity for *CovS* on *CovR* is found with regard to the *hasA* gene, which is part of the *hasABC* operon that provides the capsular material, HA, to certain GAS strains (60). We confirm that *hasA* expression is repressed in the WT-*CovRS* strains, WT-NS931 and AP53/*CovS^{WT}*, and is derepressed in strains with the particular *CovS* mutant that we find naturally in WT-AP53 or that we have engineered in strain NS931/*CovS^M*. This mutation leads to higher levels of HA in these latter two strains, along with an increase in capsular material. Similar findings have been made with respect to SK expression.

The assembly of hPg on bacterial surfaces facilitates its activation to the protease, hPm, by bacterially secreted SK, and it protects hPm from inhibition by the host plasma inhibitor, α_2 -antiplasmin. This mechanism of cell surface hPm assembly thereby allows the bacteria assembly to possess a broad spectrum protease, which, in-turn, can degrade fibrin, as well as extracellular matrices, both directly and through activation of matrix metalloproteinases (61), thereby disrupting barriers that potentially inhibit bacterial dissemination. By expression of the protein product of the *pam* gene, hPg is able to bind directly to the surface of the microorganism and, after activation, to generate this highly focalized proteolytic activity. This feature is an important characteristic of skin-tropic GAS strains, wherein PAM and PAM-related proteins are present (56). In several other GAS lines, *e.g.* the globally disseminated M1T1 and the closely related SF370 (62) strains, M-proteins do not bind hPg directly but have the ability to bind fibrinogen (63), which then serves as a template for hPg binding and activation. Interestingly, the nature of the SK produced also coordinates with the Pg binding properties of the M-proteins. AP53 and analogous strains containing functional PAM, produces SK2b, which maximally activates Pg bound to PAM via the kringle 2 region of hPg. Strains with fibrinogen-binding M-proteins, *e.g.* SF370, can assemble hPg via the Pg-kringle 1/kringle 4 domains and produce SK2a. GAS strains that contain M-proteins that cannot directly or indirectly assemble hPg (*e.g.* NS931), produce SK1, which maximally activates hPg in solution. Thus, GAS is a highly coordinated organism with respect to host-specific infection, and many strains rely in various ways on an intact fibrinolytic system, and strong trends are present that hPg assembly on GAS is necessary, but not sufficient, for GAS invasiveness. This general trend is also reflected in the lethality induced by intradermal injection of GAS lines, in a murine model of bacterial dissemination. The GAS lines that do not contain PAM, *e.g.* NS931, or are engineered not to produce PAM, *e.g.* AP53/ Δ PAM and AP53/ Δ Mga, are less invasive than lines that express PAM, *e.g.* WT-AP53. Interestingly, when the inactivating mutation of *CovS* found in WT-AP53 was restored to *CovS^{WT}*, the lethality of WT-AP53 was reversed. This could be related to the fact that hPg activation was also attenuated in this strain, although hPg binding was unaffected, and the fact that aSpeB expression is up-regulated and not down-regulated by genetic switching in this strain. In the early stages of development, aSpeB assists in colonization, and this enzyme should

therefore inhibit dissemination because of its inactivation by proteolysis of PAM and SK.

Although the major hPg receptor-binding site on *S. pyogenes* is PAM (11), other hPg receptors are also present in bacterial strains, e.g. PLR (12) and SEN (13). However, these receptors do not appear to play major roles in hPg binding or activation by SK in strains that also contain PAM or PAM-like proteins. This is shown through the nonproductive, with regard to SK2b stimulation, and low binding capacity of hPg to strains wherein PAM is absent or down-regulated, e.g. WT-NS931, AP53/ Δ Mga, AP53/ Δ PAM, despite the fact that all these strains contain SEN and PLR.

Invasive GAS infections and related sequela account for morbidity and mortality of nearly 1 million humans/year (64), and thus are serious worldwide health risks. Counteracting these potential infections with vaccines is a goal that has not been effectively achieved as yet. Thus, it is critical to identify and understand the regulatory properties of genes that have evolved to render these bacteria so effective and specific for the human host.

REFERENCES

- Smeesters, P. R., McMillan, D. J., and Sriprakash, K. S. (2010) The streptococcal M protein. A highly versatile molecule. *Trends Microbiol.* **18**, 275–282
- Perez-Casal, J., Caparon, M. G., and Scott, J. R. (1991) Mry, a trans-acting positive regulator of the M protein gene of *Streptococcus pyogenes* with similarity to the receptor proteins of two-component regulatory systems. *J. Bacteriol.* **173**, 2617–2624
- Hondorp, E. R., and McIver, K. S. (2007) The Mga virulence regulon: infection where the grass is greener. *Mol. Microbiol.* **66**, 1056–1065
- Stenberg, L., O'Toole, P., and Lindahl, G. (1992) Many group A streptococcal strains express two different immunoglobulin-binding proteins, encoded by closely linked genes. Characterization of the proteins expressed by four strains of different M-type. *Mol. Microbiol.* **6**, 1185–1194
- Simpson, W. J., LaPenta, D., Chen, C., and Cleary, P. P. (1990) Coregulation of type 12 M protein and streptococcal C5a peptidase genes in group A streptococci: evidence for a virulence regulon controlled by the virR locus. *J. Bacteriol.* **172**, 696–700
- Roberts, S. A., Churchward, G. G., and Scott, J. R. (2007) Unraveling the regulatory network in *Streptococcus pyogenes*. The global response regulator CovR represses rivR directly. *J. Bacteriol.* **189**, 1459–1463
- Bisno, A. L., Brito, M. O., and Collins, C. M. (2003) Molecular basis of group A streptococcal virulence. *Lancet Infect. Dis.* **3**, 191–200
- Kalia, A., and Bessen, D. E. (2004) Natural selection and evolution of streptococcal virulence genes involved in tissue-specific adaptations. *J. Bacteriol.* **186**, 110–121
- Lähteenmäki, K., Kuusela, P., and Korhonen, T. K. (2001) Bacterial plasminogen activators and receptors. *FEMS Microbiol. Rev.* **25**, 531–552
- McKay, F. C., McArthur, J. D., Sanderson-Smith, M. L., Gardam, S., Currie, B. J., Sriprakash, K. S., Fagan, P. K., Towers, R. J., Batzloff, M. R., Chhatwal, G. S., Ranson, M., and Walker, M. J. (2004) Plasminogen binding by group A streptococcal isolates from a region of hyperendemicity for streptococcal skin infection and a high incidence of invasive infection. *Infect. Immun.* **72**, 364–370
- Berge, A., and Sjöbring, U. (1993) PAM, a novel plasminogen-binding protein from *Streptococcus pyogenes*. *J. Biol. Chem.* **268**, 25417–25424
- Winram, S. B., and Lottenberg, R. (1996) The plasmin-binding protein Plr of group A streptococci is identified as glyceraldehyde-3-phosphate dehydrogenase. *Microbiology* **142**, 2311–2320
- Pancholi, V., and Fischetti, V. A. (1998) α -Enolase, a novel strong plasminogen binding protein on the surface of pathogenic streptococci. *J. Biol. Chem.* **273**, 14503–14515
- Churchward, G. (2007) The two faces of Janus. Virulence gene regulation by CovR/S in group A streptococci. *Mol. Microbiol.* **64**, 34–41
- Kondo, H., Nakagawa, A., Nishihira, J., Nishimura, Y., Mizuno, T., and Tanaka, I. (1997) *Escherichia coli* positive regulator OmpR has a large loop structure at the putative RNA polymerase interaction site. *Nat. Struct. Biol.* **4**, 28–31
- Dalton, T. L., and Scott, J. R. (2004) CovS inactivates CovR and is required for growth under conditions of general stress in *Streptococcus pyogenes*. *J. Bacteriol.* **186**, 3928–3937
- Gryllos, I., Levin, J. C., and Wessels, M. R. (2003) The CsrR/CsrS two-component system of group A *Streptococcus* responds to environmental Mg^{2+} . *Proc. Natl. Acad. Sci. U.S.A.* **100**, 4227–4232
- Alves, R., and Savageau, M. A. (2003) Comparative analysis of prototype two-component systems with either bifunctional or monofunctional sensors. Differences in molecular structure and physiological function. *Mol. Microbiol.* **48**, 25–51
- Wistedt, A. C., Kotarsky, H., Marti, D., Ringdahl, U., Castellino, F. J., Schaller, J., and Sjöbring, U. (1998) Kringle 2 mediates high affinity binding of plasminogen to an internal sequence in streptococcal surface protein PAM. *J. Biol. Chem.* **273**, 24420–24424
- Ben Nasr, A., Wistedt, A., Ringdahl, U., and Sjöbring, U. (1994) Streptokinase activates plasminogen bound to human group C and G streptococci through M-like proteins. *Eur. J. Biochem.* **222**, 267–276
- Bessen, D. E., Sotir, C. M., Readdy, T. L., and Hollingshead, S. K. (1996) Genetic correlates of throat and skin isolates of group A streptococci. *J. Infect. Dis.* **173**, 896–900
- Sanderson-Smith, M. L., Dinkla, K., Cole, J. N., Cork, A. J., Maamary, P. G., McArthur, J. D., Chhatwal, G. S., and Walker, M. J. (2008) M protein-mediated plasminogen binding is essential for the virulence of an invasive *Streptococcus pyogenes* isolate. *FASEB J.* **22**, 2715–2722
- Roberts, S. A., and Scott, J. R. (2007) RivR and the small RNA RivX: the missing links between the CovR regulatory cascade and the Mga regulon. *Mol. Microbiol.* **66**, 1506–1522
- Schmittgen, T. D., and Livak, K. J. (2008) Analyzing real-time PCR data by the comparative C_T method. *Nat. Protoc.* **3**, 1101–1108
- Enright, M. C., Spratt, B. G., Kalia, A., Cross, J. H., and Bessen, D. E. (2001) Multilocus sequence typing of *Streptococcus pyogenes* and the relationships between emm type and clone. *Infect. Immun.* **69**, 2416–2427
- Cole, J. N., McArthur, J. D., McKay, F. C., Sanderson-Smith, M. L., Cork, A. J., Ranson, M., Rohde, M., Itzek, A., Sun, H., Ginsburg, D., Kotb, M., Nizet, V., Chhatwal, G. S., and Walker, M. J. (2006) Trigger for group A streptococcal M1T1 invasive disease. *FASEB J.* **20**, 1745–1747
- Zhang, Y., Liang, Z., Hsueh, H. T., Ploplis, V. A., and Castellino, F. J. (2012) Characterization of streptokinases from group A streptococci reveals a strong functional relationship that supports the coinheritance of plasminogen-binding M protein and cluster 2b streptokinase. *J. Biol. Chem.* **287**, 42093–42103
- Nilsen, S. L., and Castellino, F. J. (1999) Expression of human plasminogen in *Drosophila* Schneider S2 cells. *Protein Expr. Purif.* **16**, 136–143
- Hytönen, J., Haataja, S., Gerlach, D., Podbielski, A., and Finne, J. (2001) The SpeB virulence factor of *Streptococcus pyogenes*, a multifunctional secreted and cell surface molecule with streptadhesin, laminin-binding and cysteine protease activity. *Mol. Microbiol.* **39**, 512–519
- Zimmerlein, B., Park, H. S., Li, S., Podbielski, A., and Cleary, P. P. (2005) The M protein is dispensable for maturation of streptococcal cysteine protease SpeB. *Infect. Immun.* **73**, 859–864
- Schrager, H. M., Rheinwald, J. G., and Wessels, M. R. (1996) Hyaluronic acid capsule and the role of streptococcal entry into keratinocytes in invasive skin infection. *J. Clin. Invest.* **98**, 1954–1958
- Sun, H., Ringdahl, U., Homeister, J. W., Fay, W. P., Engleberg, N. C., Yang, A. Y., Rozek, L. S., Wang, X., Sjöbring, U., and Ginsburg, D. (2004) Plasminogen is a critical host pathogenicity factor for group A streptococcal infection. *Science* **305**, 1283–1286
- Ringdahl, U., Svensson, M., Wistedt, A. C., Renné, T., Kellner, R., Müller-Esterl, W., and Sjöbring, U. (1998) Molecular co-operation between protein PAM and streptokinase for plasmin acquisition by *Streptococcus pyogenes*. *J. Biol. Chem.* **273**, 6424–6430
- Liang, Z., Breman, A. M., Grimes, B. R., and Rosen, E. D. (2008) Identifying and genotyping transgene integration loci. *Transgenic Res.* **17**, 979–983

35. Kreikemeyer, B., McIver, K. S., and Podbielski, A. (2003) Virulence factor regulation and regulatory networks in *Streptococcus pyogenes* and their impact on pathogen-host interactions. *Trends Microbiol.* **11**, 224–232
36. Ferretti, J. J., McShan, W. M., Ajdic, D., Savic, D. J., Savic, G., Lyon, K., Primeaux, C., Sezate, S., Suvorov, A. N., Kenton, S., Lai, H. S., Lin, S. P., Qian, Y., Jia, H. G., Najar, F. Z., Ren, Q., Zhu, H., Song, L., White, J., Yuan, X., Clifton, S. W., Roe, B. A., and McLaughlin, R. (2001) Complete genome sequence of an M1 strain of *Streptococcus pyogenes*. *Proc. Natl. Acad. Sci. U.S.A.* **98**, 4658–4663
37. Cnudde, S. E., Prorok, M., Castellino, F. J., and Geiger, J. H. (2006) X-ray crystallographic structure of the angiogenesis inhibitor, angiostatin, bound to a peptide from the group A streptococcal surface protein PAM. *Biochemistry* **45**, 11052–11060
38. Fu, Q., Figuera-Losada, M., Ploplis, V. A., Cnudde, S., Geiger, J. H., Prorok, M., and Castellino, F. J. (2008) The lack of binding of VEK-30, an internal peptide from the group A streptococcal M-like protein, PAM, to murine plasminogen is due to two amino acid replacements in the plasminogen kringle-2 domain. *J. Biol. Chem.* **283**, 1580–1587
39. Schenone, M. M., Warder, S. E., Martin, J. A., Prorok, M., and Castellino, F. J. (2000) An internal histidine residue from the bacterial surface protein, PAM, mediates its binding to the kringle-2 domain of human plasminogen. *J. Pept. Res.* **56**, 438–445
40. Podbielski, A. (1993) Three different types of organization of the vir regulon in group A streptococci. *Mol. Gen. Genet.* **237**, 287–300
41. Levin, J. C., and Wessels, M. R. (1998) Identification of *csrR/csrS*, a genetic locus that regulates hyaluronic acid capsule synthesis in group A *Streptococcus*. *Mol. Microbiol.* **30**, 209–219
42. Heath, A., DiRita, V. J., Barg, N. L., and Engleberg, N. C. (1999) A two-component regulatory system, *CsrR-CsrS*, represses expression of three *Streptococcus pyogenes* virulence factors, hyaluronic acid capsule, streptolysin S, and pyrogenic exotoxin B. *Infect. Immun.* **67**, 5298–5305
43. Treviño, J., Perez, N., Ramirez-Peña, E., Liu, Z., Shelburne, S. A., 3rd, Musser, J. M., and Sumbly, P. (2009) CovS simultaneously activates and inhibits the CovR-mediated repression of distinct subsets of group A *Streptococcus* virulence factor-encoding genes. *Infect. Immun.* **77**, 3141–3149
44. Hauser, A. R., Stevens, D. L., Kaplan, E. L., and Schlievert, P. M. (1991) Molecular analysis of pyrogenic exotoxins from *Streptococcus pyogenes* isolates associated with toxic shock-like syndrome. *J. Clin. Microbiol.* **29**, 1562–1567
45. Federle, M. J., and Scott, J. R. (2002) Identification of binding sites for the group A streptococcal global regulator CovR. *Mol. Microbiol.* **43**, 1161–1172
46. Churchward, G., Bates, C., Gusa, A. A., Stringer, V., and Scott, J. R. (2009) Regulation of streptokinase expression by CovR/S in *Streptococcus pyogenes*. CovR acts through a single high affinity binding site. *Microbiology* **155**, 566–575
47. Rezcallah, M. S., Boyle, M. D., and Sledjeski, D. D. (2004) Mouse skin passage of *Streptococcus pyogenes* results in increased streptokinase expression and activity. *Microbiology* **150**, 365–371
48. Cole, J. N., Pence, M. A., von Köckritz-Blickwede, M., Hollands, A., Gallo, R. L., Walker, M. J., and Nizet, V. (2010) M protein and hyaluronic acid capsule are essential for *in vivo* selection of covRS mutations characteristic of invasive serotype M1T1 group A *Streptococcus*. *MBio.* **1**, e00191–10
49. Walker, M. J., Hollands, A., Sanderson-Smith, M. L., Cole, J. N., Kirk, J. K., Henningham, A., McArthur, J. D., Dinkla, K., Aziz, R. K., Kansal, R. G., Simpson, A. J., Buchanan, J. T., Chhatwal, G. S., Kotb, M., and Nizet, V. (2007) DNase Sda1 provides selection pressure for a switch to invasive group A streptococcal infection. *Nat. Med.* **13**, 981–985
50. Haanes, E. J., Heath, D. G., and Cleary, P. P. (1992) Architecture of the vir regulons of group A streptococci parallels opacity factor phenotype and M protein class. *J. Bacteriol.* **174**, 4967–4976
51. Podbielski, A., Flösdorf, A., and Weber-Heinemann, J. (1995) The group A streptococcal virR49 gene controls expression of four structural vir regulon genes. *Infect. Immun.* **63**, 9–20
52. McIver, K. S., Heath, A. S., Green, B. D., and Scott, J. R. (1995) Specific binding of the activator Mga to promoter sequences of the *emm* and *scpA* genes in the group A *Streptococcus*. *J. Bacteriol.* **177**, 6619–6624
53. Ribardo, D. A., and McIver, K. S. (2006) Defining the Mga regulon. Comparative transcriptome analysis reveals both direct and indirect regulation by Mga in the group A *Streptococcus*. *Mol. Microbiol.* **62**, 491–508
54. Gardiner, D., Hartas, J., Currie, B., Mathews, J. D., Kemp, D. J., and Sriprakash, K. S. (1995) Vir typing: a long-PCR typing method for group A streptococci. *PCR Methods Appl.* **4**, 288–293
55. Sanderson-Smith, M. L., Walker, M. J., and Ranson, M. (2006) The maintenance of high affinity plasminogen binding by group A streptococcal plasminogen-binding M-like protein is mediated by arginine and histidine residues within the a1 and a2 repeat domains. *J. Biol. Chem.* **281**, 25965–25971
56. Svensson, M. D., Sjöbring, U., and Bessen, D. E. (1999) Selective distribution of a high affinity plasminogen-binding site among group A streptococci associated with impetigo. *Infect. Immun.* **67**, 3915–3920
57. Federle, M. J., McIver, K. S., and Scott, J. R. (1999) A response regulator that represses transcription of several virulence operons in the group A *Streptococcus*. *J. Bacteriol.* **181**, 3649–3657
58. Engleberg, N. C., Heath, A., Miller, A., Rivera, C., and DiRita, V. J. (2001) Spontaneous mutations in the *CsrRS* two-component regulatory system of *Streptococcus pyogenes* result in enhanced virulence in a murine model of skin and soft tissue infection. *J. Infect. Dis.* **183**, 1043–1054
59. Graham, M. R., Smoot, L. M., Migliaccio, C. A., Virtaneva, K., Sturdevant, D. E., Porcella, S. F., Federle, M. J., Adams, G. J., Scott, J. R., and Musser, J. M. (2002) Virulence control in group A *Streptococcus* by a two-component gene regulatory system. Global expression profiling and *in vivo* infection modeling. *Proc. Natl. Acad. Sci. U.S.A.* **99**, 13855–13860
60. Bernish, B., and van de Rijn, I. (1999) Characterization of a two-component system in *Streptococcus pyogenes* which is involved in regulation of hyaluronic acid production. *J. Biol. Chem.* **274**, 4786–4793
61. Werb, Z. (1997) ECM and cell surface proteolysis. Regulating cellular ecology. *Cell* **91**, 439–442
62. Cleary, P. P., Kaplan, E. L., Handley, J. P., Wlazlo, A., Kim, M. H., Hauser, A. R., and Schlievert, P. M. (1992) Clonal basis for resurgence of serious *Streptococcus pyogenes* disease in the 1980s. *Lancet* **339**, 518–521
63. Schmidt, K. H., and Wadström, T. (1990) A secreted receptor related to M1 protein of *Streptococcus pyogenes* binds to fibrinogen, IgG, and albumin. *Zentralbl. Bakteriol.* **273**, 216–228
64. Carapetis, J. R., Steer, A. C., Mulholland, E. K., and Weber, M. (2005) The global burden of group A streptococcal diseases. *Lancet Infect. Dis.* **5**, 685–694